

INVITED TALK GIVEN
 AT THE 44TH WORKSHOP ON 'QCD AT COSMIC ENERGIES:
 THE HIGHEST ENERGY COSMIC RAYS AND QCD',
 ERICE, ITALY, AUG 29 - SEP 5, 2004
 (TO BE PUBLISHED IN THE PROCEEDINGS)

THE ANTARES EXPERIMENT: PAST, PRESENT AND FUTURE

IGOR SOKALSKI

ON BEHALF OF THE ANTARES COLLABORATION *

*INFN / Bari
 via Amendola 173
 I-70126 Bari
 Italia*

E-mail: Igor.Sokalski@ba.infn.it

The ANTARES collaboration aims to build a deep underwater Cherenkov neutrino telescope in the Mediterranean Sea at 2500 m depth, about 40 km off-shore of La Seyne sur Mer, near Toulon (42°50' N, 6°10' E). The collaboration was formed in 1996 and the experiment is currently in the construction phase. The final ANTARES detector, consisting of 12 strings each equipped with 75 photomultiplier tubes, is planned to be fully deployed and taking data by 2007. The project aims to detect atmospheric and extraterrestrial neutrinos with energies above $E_\nu \sim 10$ GeV by means of the Cherenkov light that is generated in water by charged particles which are produced in the neutrino interactions.

1. Introduction

Neutrinos are an attractive tool for astrophysical investigations since they are weakly interacting and hence they are not absorbed in sources or during propagation to the Earth (moreover, being neutral, they are not deflected by magnetic fields). Nevertheless, due to the same property, huge volume neutrino detectors are needed. ANTARES is one of the several on-going projects ¹⁻⁶ on underwater/ice neutrino telescopes.

The idea to construct large deep underwater Cherenkov detectors for neutrino astronomy using natural basins was formulated by M. A. Markov in 1960 ⁷ as an alternative to the underground neutrino telescopes whose sensitivity does not allow to detect neutrinos from the cosmic accelerators. The effective area of the cosmic neutrino detector must be at least of the order of 0.1-1 km² which goes far beyond the constructional possibilities of

*<http://www.slac.stanford.edu/spires/find/experiments/www2?expt=antares>

the underground technique. The underwater/ice neutrino telescopes aim to detect neutrinos with energies above $E_\nu \sim 10 \text{ GeV}$ by means of the detection of the Cherenkov light that is generated in water by charged particles which are produced in neutrino interactions. Water (or ice) serves for three purposes: it represents *i)* a shield which protects from atmospheric muon background, *ii)* a target in which neutrino interaction occurs and *iii)* the detection medium where the Cherenkov light is emitted and propagates. The Cherenkov photons are detected by a 3D grid of photomultipliers (PMTs) immersed deep (at the km scale depth) under water or ice. The typical detector consists of vertical lines (strings) equipped with PMTs and spaced by 10-100 m from each other. The neutrino direction can be reconstructed using times and position of hit PMTs, the energy is estimated using the amplitude information.

As a matter of fact, neutrinos oscillate during their propagation from sources, hence signal from sources should consist of all neutrino flavors. However, neutrino telescopes were originally optimized for the detection of muon neutrinos through the reaction $\nu_\mu N \xrightarrow{CC} \mu X$, since muons propagate through large distances increasing the 'effective' target mass of the detector (for 1 TeV muon, *e.g.*, the mean range is about 2.5 km w.e.). Moreover, muon tracks can be reconstructed with good angular resolution allowing to point-back to neutrino sources. On the other hand, detection of shower events (which are produced in the detector sensitive volume by ν_e 's, ν_τ with energies lower than $E_{\nu_\tau} \sim 1 \text{ PeV}$ and neutral current interactions) has also interesting potentials, as discussed, *e.g.*, in ^{8,9}, as well as detection of extremely high energy ν_τ 's through τ -leptons whose ranges at PeV and EeV energy range are compatible with muon ones (see, *e.g.*, ^{10,11}). In a narrow energy range around 6.33 PeV the resonant processes $\bar{\nu}_e e^- \rightarrow W^-(Z^0) \rightarrow X$ (where X can be $\bar{\nu}_e e^-$, $\bar{\nu}_\mu \mu^-$, $\bar{\nu}_\tau \tau^-$ or hadrons) ¹²⁻¹⁴ which result both in 'shower' and 'track' events must be taken into account, as well.

The ANTARES ^a Collaboration was formed in 1996. By that time the pioneering underwater neutrino project DUMAND in the Pacific Ocean ¹⁵ had been cancelled, the BAIKAL detector in the Siberian lake Baikal had reported the first atmospheric neutrinos detected underwater ^{3,16}, the AMANDA-B ¹⁷ detector at the South Pole was under construction (AMANDA-A ¹⁸ had been taking data for 2 years) and the NESTOR experiment ⁶ in the Mediterranean Sea near Pinos (Greece) was at the R&D phase.

^aANTARES = Astronomy with a Neutrino Telescope and Abbyss environmental Research.

Now the ANTARES project joins about 200 scientists and engineers from France, Germany, Italy, Russia, Spain, The Netherlands and the United Kingdom. After an extensive R&D program the collaboration entered the phase of construction of a 12-string neutrino telescope in the Mediterranean Sea at 2500 m depth. Given the presence of AMANDA¹ and ICECUBE⁴ at the South Pole, a detector in the Mediterranean will allow to cover the whole sky looking for extraterrestrial neutrino sources.

2. The Past

2.1. Site investigation

In 1996-99 an intense R&D program was performed. The deployment and recovery technologies, electronics and mechanical structures were developed and tested with more than 30 deployments of autonomous strings. The environmental properties at the detector site were investigated^{19–21}.

Concerning the optical backgrounds it was found that PMT counting rates have very strong temporal variations due to bioluminescence organisms (see Figure 1). The baseline rate slowly varies between 50 kHz and 300 kHz on a 10" PMT being accompanied by short (from several seconds to several minutes) several hundred kHz bioluminescence ‘bursts’. Nevertheless, the measured optical background is 50-70% of the time below 100 kHz which is a rate acceptable for data taking. To suppress the high optical backgrounds, coincidence requirements and PMT thresholds higher than 0.25 photo-electrons will be used during data taking, which will slightly reduce the efficiency at low energies without deteriorating it in the region of interest for astrophysical sources ($E_\nu > 100$ GeV).

Light transmission loss for glass containers that house PMTs was found strong in long-term tests for up-looking surfaces. It led to the decision to turn all PMTs downward. Signal loss due to bio-fouling and sedimentation was measured to be 1.6% after 8 months at equator of glass sphere saturating with time.

The optical properties of water at the experiment site were measured during several years. The effective attenuation length varies in a range $40 \text{ m} < \Lambda_{att} < 60 \text{ m}$ (see Figure 2) while the effective scattering length is $\Lambda_{scatt} > 200 \text{ m}$ for blue light ($\lambda = 466 \text{ nm}$). Only 5% of the photons emitted by an isotropic source located 24 m from a PMT are collected out of a 10 ns time window being delayed due to scattering. This allows a good time resolution needed for event reconstruction.

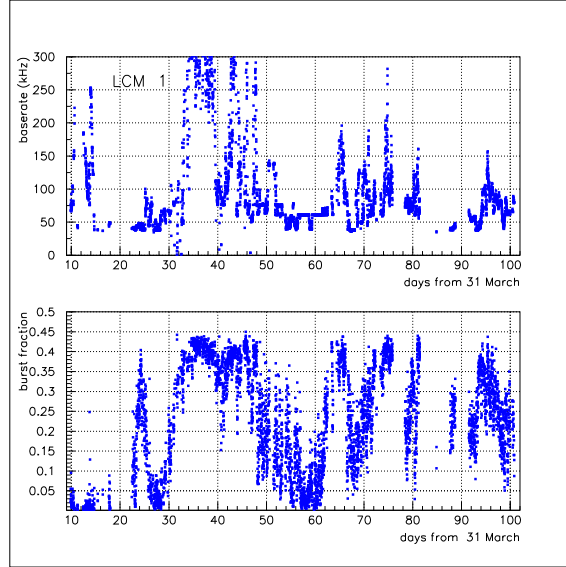


Figure 1. Summary of counting rate in 3 PMTs during 65 days in April–May, 2003 vs time. Top panel: the average baseline rate. Bottom panel: the fraction of time the rate is significantly higher than this average baseline rate (burst fraction).

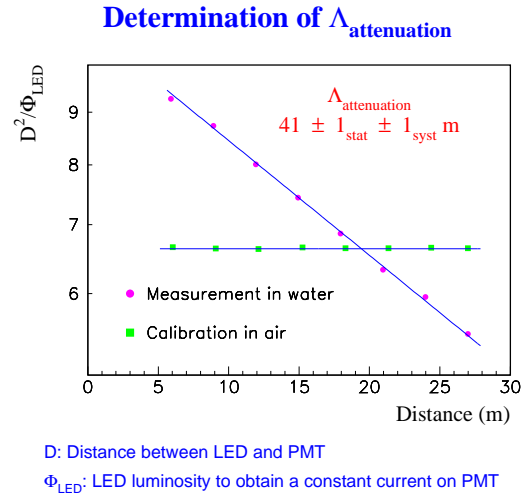


Figure 2. Determination of the effective attenuation length from the setup immersed in December 1997.

2.2. *Prototype strings*

Several prototype strings were immersed deep in the sea and operated in the frame of the ANTARES R&D program.

Firstly, a 350 m length ‘demonstrator string’ instrumented with 7 PMTs was deployed at a depth of 1100 m, 40 km off the coast of Marseille and operated for 8 months (November 1999 - July 2000). The string was controlled and read out via a ~ 40 km-long electro-optical cable connected to the shore station. It allowed to test the deployment procedure with a full-scale string, positioning system and collect $\sim 5 \cdot 10^4$ seven-fold coincidences from atmospheric muons. Relative distances were measured with an accuracy of ~ 5 cm and accuracy of absolute positioning was ~ 1 m. The angular distribution of atmospheric muons was reproduced reasonably (Figure 3) and the fraction of multi-muon events was found to be about 50% which is in agreement with expectation for such a shallow depth as 1100 m.

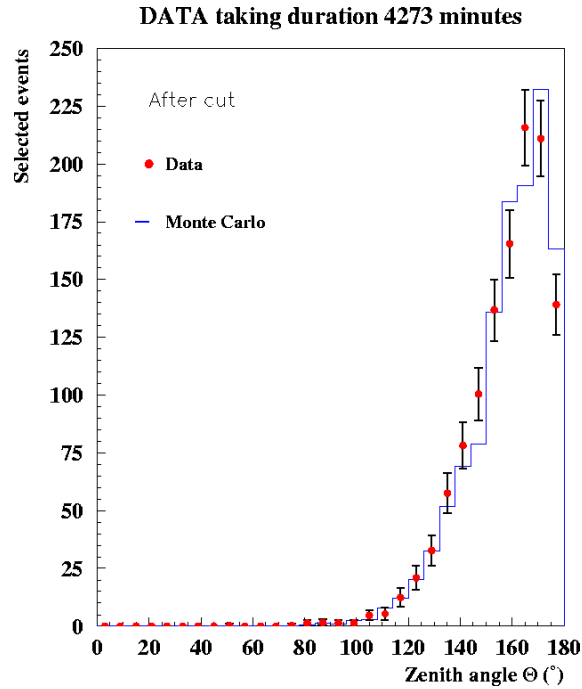


Figure 3. Reconstructed angular distribution from the ‘demonstrator string’ data. The areas of the curves are normalized to each other.

Then in December 2002 and February 2003 the prototype and the mini instrumentation lines²² have been deployed and positioned on sea bed within a few meters from their nominal positions. In March 2003 a manned submarine 'Nautil' successfully connected both lines to the electro-optical cable. The data have been taken continuously until the recovery of the prototype line in July 2003 and analyzed to study the optical background at the ANTARES site. Two problems occurred in the prototype tests. A water leak developed in one of the electronic containers due to a faulty supplier specification for a connector. This made further operation impossible and the line was recovered in May 2003. Also, a defect in the clock signal transmission caused by a broken optical fiber inside the line meant that data with timing information at nanosecond precision were unavailable. Nevertheless, during about 100 days of the prototype line operation data were recorded, both on the functionality of the detector and on environmental conditions.

3. The Present

3.1. The ANTARES 12-string detector: design

After R&D experience, the collaboration moved to the next stage: construction of a 12-string detector which can be considered as a step toward a 1 km³ detector. The design of the planned detector is shown in Figure 4. Strings are anchored at the sea floor and held taut by buoys. Each string

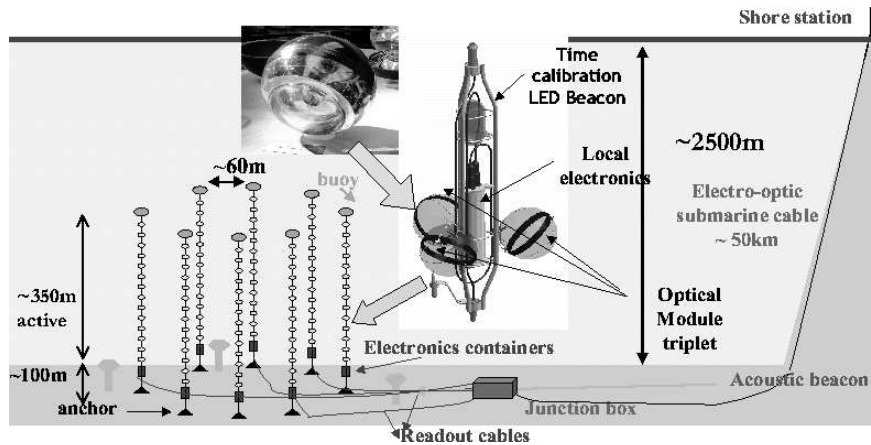


Figure 4. Schematic view of the ANTARES 12-string detector.

is instrumented with 75 optical modules (OMs) ²³ containing 10“ Hamamatsu R7081-20 PMTs ²⁴ housed in glass spheres. The main specifications that ANTARES PMTs must satisfy are: a transit time spread of less than 3 ns (FWHM), a peak to valley ratio larger than 2, a dark count of less than 20 kHz for a 0.25 photo-electron threshold, and a gain larger than $5 \cdot 10^7$ for high voltage lower than 2000 V. Laser calibrations in a dark room using a prototype line made of 5 storeys have shown that, after corrections of clock delays between consecutive storeys, the achievable timing resolution is $\sigma \sim 0.9 - 1.2$ ns. OMs are grouped in triplets at 25 levels separated by 14.5 m. 3 PMTs in each triplet are oriented at 45° to the nadir. Strings are separated from each other by $\sim 60-70$ m. All the strings are connected to a ‘junction box’ by means of electro-optical link cables. The junction box is connected to the shore station by a 50 km long 48-fiber electro-optical cable (which was deployed in October 2001). PMT signals are processed by Analogue Ring Samplers which measure the arrival time and charge for 1 p.e.-pulses (99% of the pulses) and perform wave form digitization for larger amplitudes. Digitized data from each OM are sent to shore (~ 1 GB/s/detector). The data flow is reduced down to ~ 1 MB/s on the shore by means of an on-shore data filter ²⁵. A 100 PC farm is foreseen on shore to process and collect the data. The telescope will be complemented with an instrumentation string for hydrological parameter measurements and for calibration purposes. The deployment of the detector is planned for 2005-2007.

3.2. The 12-string detector: physical performance

The main background for deep underwater Cherenkov experiments comes from atmospheric muons. To suppress this background one selects the ‘ ν_μ events’ only out of events that have been reconstructed as up-going ones.

Figure 5 shows the neutrino effective area for the 12-string ANTARES detector for different nadir angles. The neutrino effective area is the sensitive area of the detector ‘seen’ by neutrinos producing detectable muons when entering the Earth. Since cross section of ν - N charged current interactions (in which muons are produced) is very small, the neutrino effective area is orders of magnitude lower compared to geometrical dimensions of the detector. The decrease of the area in the vertical region at high energies is due to the Earth shadowing effect which is remarkable for neutrino energies larger than $E_\nu \sim 50$ TeV (see, *e.g.*, ²⁶).

The angular resolution as obtained with the ANTARES simulation is

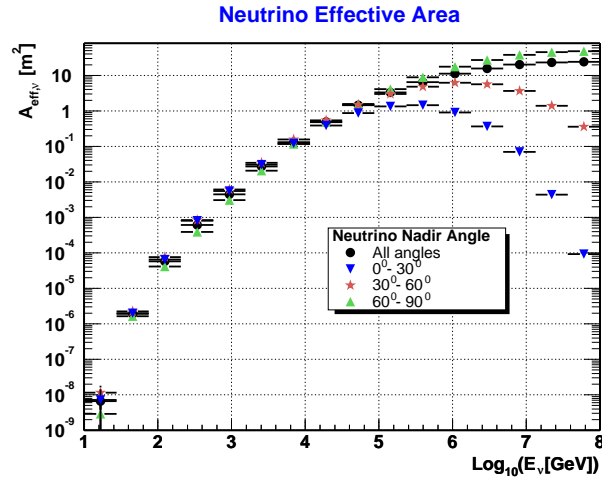


Figure 5. The neutrino effective area for 12-string ANTARES detector computed for different nadir angles vs neutrino energy.

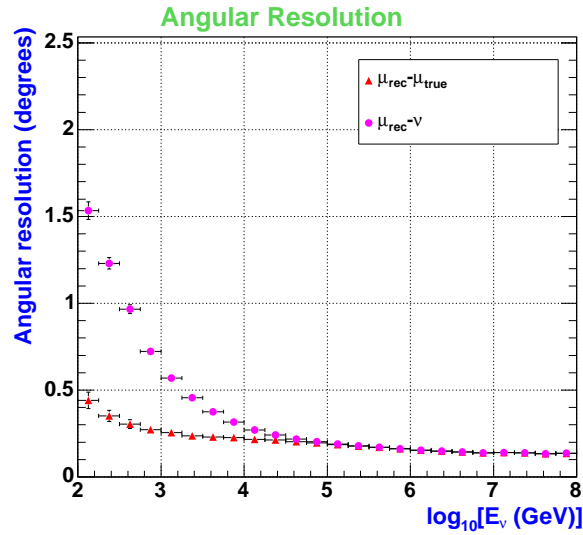


Figure 6. ANTARES angular resolution vs neutrino energy. The dots: median angle between the simulated neutrino and reconstructed muon direction. Triangles: the median of the angle between the simulated muon and reconstructed one.

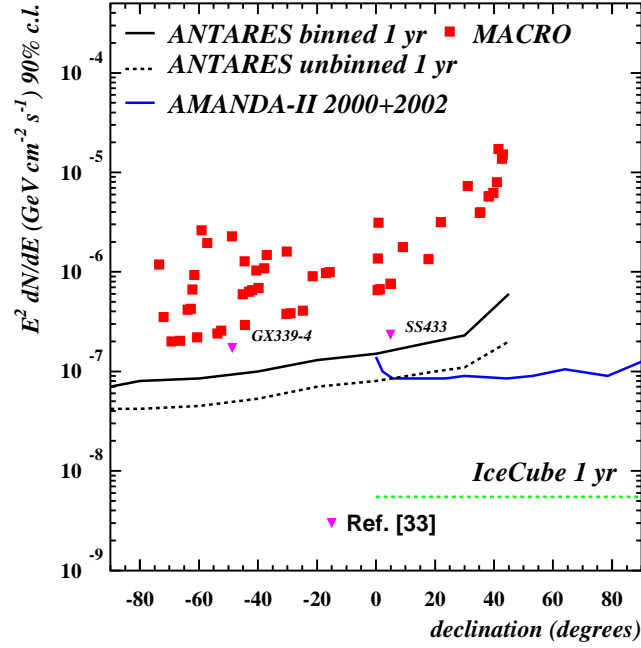


Figure 7. Upper limits (90% CL) on E^{-2} neutrino fluxes as a function of the source declination for MACRO²⁸, expected sensitivity of AMANDA-II corresponding to 2000-2002 data²⁹, ICECUBE³¹ and ANTARES³² (for a search method using a grid in the sky and an unbinned method based on likelihood ratio). The triangles indicates the expected neutrino flux from two persistent micro-quasars as calculated in³³.

shown in Figure 6. The plot shows the median angle between the neutrino source and the reconstructed muon (that is the pointing capability for a neutrino source) and the ‘intrinsic angular resolution’, that is the angle between the ‘true’ muon track and reconstructed one. The angular resolution of the ANTARES detector is about 0.2° for $E_\nu \geq 10$ TeV where it is limited only by PMT transit time spread and light scattering and $\sim 0.3^\circ$ – 1.5° at $E_\nu \sim 0.1$ – 10 TeV where accuracy is dominated by $\nu - \mu$ kinematics.

The sky coverage for the ANTARES detector is 3.5π sr with the whole Southern hemisphere observable. Promising neutrino source candidates as, *e.g.*, the Galactic Center and supernova remnant RX J1713.7-3946²⁷ are visible 67% and 78% of the time, correspondingly. The instantaneous overlap with South Pole detectors AMANDA¹ and ICECUBE⁴ is 0.5π sr

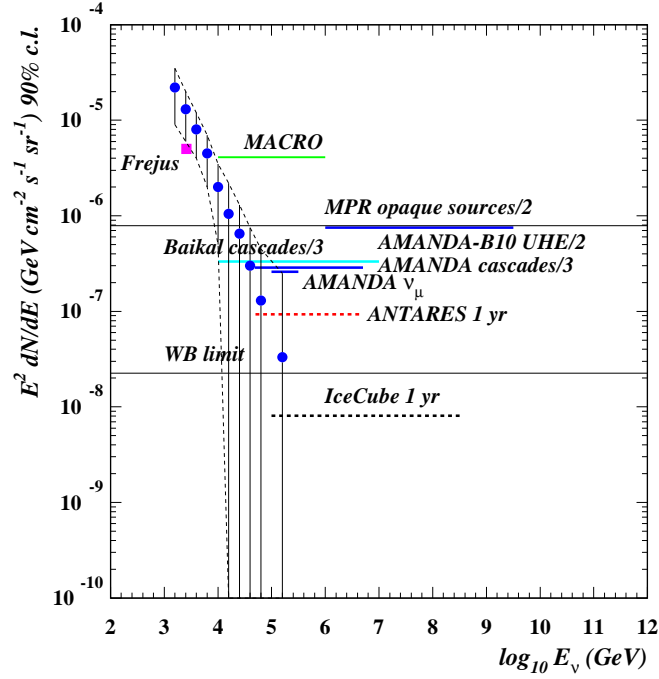


Figure 8. Sensitivity for ANTARES to the diffuse neutrino flux compared to 90% c.l. limits on diffuse E^{-2} fluxes of $\nu_\mu + \bar{\nu}_\mu$ in the hypothesis of ν oscillations as measured by AMANDA-II³⁰, BAIKAL³⁴, MACRO³⁵ and FREJUS³⁶. Limits for other flavors than ν_μ (cascades) have been divided by the number of contributing flavors. Sensitivity of ICECUBE³¹ is shown, as well. Dots are the measured atmospheric neutrino flux by AMANDA-II³⁷. Waxmann & Bahcall limit on diffuse neutrino flux³⁸ and Mannheim-Protheroe-Rachen limit on diffuse neutrino flux for opaque sources³⁹ are given by thin horizontal lines.

with 1.5π sr common view per day.

The sensitivity of ANTARES for 1 year of data taking as a function of declination for two different methods of searches for point-like sources is shown in Figure 7, where it is compared to other experiments. It can be seen that there is a real hope to detect a signal from the most promising sources (*e.g.*, galactic micro-quasars³³).

Studies on the sensitivity of ANTARES to a diffuse muon neutrino flux from populations of sources have brought to the result given in Figure 8. The sensitivity of the detector to diffuse neutrino fluxes allows to reach Waxmann & Bahcall limit³⁸ in about 4 years.

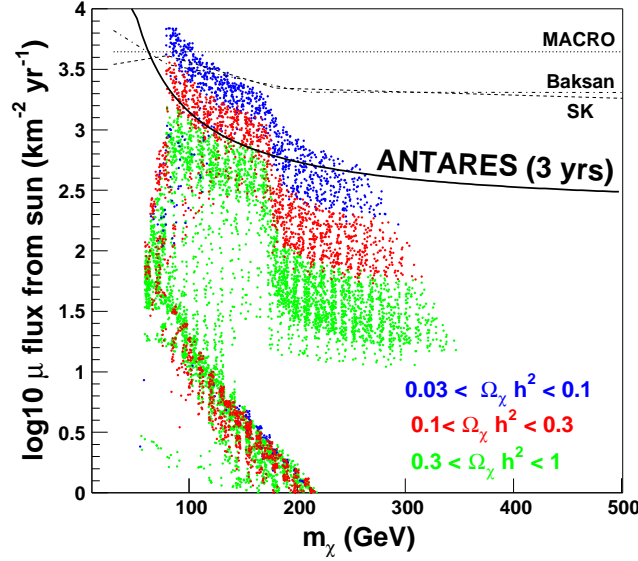


Figure 9. The ANTARES 12-string detector sensitivity to the muon flux from neutralino annihilations in the core of the Sun in comparison to the upper limits from MACRO ⁴⁰, BAKSAN ⁴¹, SUPER-KAMIOKANDE ⁴² and to predictions of mSUGRA ⁴³ models.

Apart from the neutrino astronomy, other motivations are included in the ANTARES scientific program. Neutralinos, the best candidates for cold dark matter, can be gravitationally captured in the massive astrophysical objects such as the Sun, the Earth or the Galactic Center and annihilate there producing neutrinos in the decay chain. Expected ANTARES sensitivity to the muon flux from neutralino annihilation in the core of the Sun for the case of a ‘hard’ neutrino spectrum (assuming 100% annihilations $\chi\bar{\chi} \rightarrow W^+W^-$) is shown in Figure 9.

4. The Future

The ANTARES 12-string detector can be considered as a first stage toward a km³-scale telescope, in which European institutions involved in current deep underwater neutrino telescope projects (ANTARES ², NEMO ⁵ and NESTOR ⁶) are already collaborating. This network, KM3NET ⁴⁴, will give birth to a 1 km³ Northern hemisphere telescope which will complement the ICECUBE detector ⁴ in the Southern hemisphere.

5. Conclusions

The construction of the ANTARES detector is well underway. It is planned to be fully deployed and start to take data in 2007. Calculations based on the data on environmental conditions at the experiment site and on studied properties of electronic components shows that predicted sensitivity of the detector to diffuse neutrino fluxes, point-like neutrino searches and WIMP searches is quite enough to participate in a competition with other experimental groups. The deployment of the ANTARES neutrino telescope can be considered as a step toward the deployment of a 1 km³ detector in the Mediterranean Sea.

References

1. The AMANDA experiment: E. Andres *et al.*, *Astropart. Phys.* **13**, 1 (2000) (available from <arXiv:astro-ph/9906203>); J. Ahrens *et al.*, e-print *astro-ph/0409423*. See also URL <http://amanda.uci.edu/>
2. The ANTARES experiment: E. Aslanides *et al.*, e-print *astro-ph/9907432*; E. V. Korolkova *et al.*, *Nucl. Phys. Proc. Suppl.* **136**, 69 (2004) (available from <arXiv:astro-ph/0408239>). See also URL <http://antares.in2p3.fr/>
3. The BAIKAL experiment: I. A. Belolaptikov *et al.*, *Astropart. Phys.* **7**, 263 (1997); Ch. Spiering *et al.*, *Nucl. Phys. Proc. Suppl.* **138**, 175 (2005). See also URL <http://baikal1.jinr.ru/>
4. The ICECUBE experiment: J. Alvarez-Muniz and F. Halzen, *AIP Conf. Proc.* **579**, 305 (2001) (available from <arXiv:astro-ph/0102106>); Sh. Yoshida *et al.*, *Nucl. Phys. Proc. Suppl.* **138**, 179 (2005). See also URL <http://icecube.wisc.edu/>
5. The NEMO experiment: C. N. De Marzo *et al.*, in Proceedings of the Vulcano Workshop 2000: Frontier Objects in Astrophysics and Particle Physics, Vulcano, Italy, 22-27 May 2000, p. 593; E. Migneco *et al.*, *Nucl. Phys. Proc. Suppl.* **136**, 61 (2004). See also URL <http://nemoweb.lns.infn.it/>
6. The NESTOR experiment: L. K. Resvanis *et al.*, *Nucl. Phys. Proc. Suppl.* **35**, 294 (1994); L. K. Resvanis *et al.*, *Nucl. Phys. Proc. Suppl.* **138**, 187 (2005). See also URL <http://www.nestor.org.gr/>
7. M. A. Markov, in Proceedings of 10th International Conference on High Energy and Nuclear Physics, Rochester, USA, 25 August - 1 September 1960, p. 579.
8. M. Ackermann *et al.* (The AMANDA Collaboration), *Astropart. Phys.* **22**, 127 (2004) (available from <arXiv:astro-ph/0405218>).
9. S. I. Dutta, M. H. Reno and I. Sarcevic, *Phys. Rev.* **D62**, 123001 (2000) (available from <arXiv:hep-ph/0005310>).
10. J. G. Learned and S. Pakvasa, *Astropart. Phys.* **3**, 267 (1995) (available from <arXiv:hep-ph/9405296>).
11. E. Bugaev, T. Montaruli, Yu. Shlepin and I. Sokalski, *Astropart. Phys.* **21**, 491 (2004) (available from <arXiv:hep-ph/0312295>).

12. S. L. Glashow, *Phys. Rev.* **118**, 316 (1960).
13. V. S. Berezinsky and A. Z. Gazizov, *JETP Lett.* **25**, 254 (1977).
14. K. O. Mikaelian and I. M. Zheleznykh, *Phys. Rev.* **D22**, 2122 (1980).
15. K. K. Young *et al.* (The DUMAND Collaboration), in Proceedings of Joint 15th International Lepton Photon Symposium at High Energies and European Physical Society Conference on High-energy Physics, Geneva, Switzerland, 25 July - 1 August 1991, Vol.1, p.662. See also URL <http://www.phys.hawaii.edu/dmnd/dumand.html>
16. L. B. Bezrukov *et al.* (The BAIKAL Collaboration), e-print *astro-ph/9601161*; V. A. Balkanov *et al.* (The BAIKAL Collaboration), *Astropart. Phys.* **12**, 75 (1999) (available from <arXiv:astro-ph/9903341>).
17. P. O. Hulth *et al.* (The AMANDA Collaboration), e-print *astro-ph/9612068*.
18. P. Askebjerg *et al.* (The AMANDA Collaboration), *Nucl. Phys. Proc. Suppl.* **38**, 287 (1995).
19. P. Amram *et al.* (The ANTARES Collaboration), *Astropart. Phys.* **13**, 127 (2000) (available from <arXiv:astro-ph/9910170>).
20. P. Amram *et al.* (The ANTARES Collaboration), *Astropart. Phys.* **19**, 253 (2003) (available from <arXiv:astro-ph/0206454>).
21. J. A. Aguilar *et al.* (The ANTARES Collaboration), e-print *astro-ph/0412126* (to be published in *Astropart. Phys.*).
22. M. Circella *et al.* (The ANTARES Collaboration), in Proceedings of 28th International Cosmic Ray Conference (ICRC 2003), Tsukuba, Japan, 31 July - 7 August 2003, p.1529.
23. P. Amram *et al.* (The ANTARES Collaboration), *NIM* **A484**, 369 (2002) (available from <arXiv:astro-ph/0112172>).
24. J. A. Aguilar *et al.* (The ANTARES Collaboration), to be submitted to *NIM*.
25. M. C. Bouwhuis *et al.* (The ANTARES Collaboration), in Proceedings of 28th International Cosmic Ray Conference (ICRC 2003), Tsukuba, Japan, 31 July - 7 August 2003, p.1541.
26. A. L'Abbate, T. Montaruli and I. Sokalski, e-print *hep-ph/0406133* (to be published in *Astropart. Phys.*).
27. R. Enomoto *et al.* (The CANGAROO Collaboration), *Nature*, **416**, 823 (2002).
28. M. Ambrosio *et al.* (The MACRO Collaboration), *Astrophys. J.* **546**, 1038 (2001) (available from <arXiv:astro-ph/0002492>).
29. M. Ackermann *et al.* (The AMANDA Collaboration), e-print *astro-ph/0412347* (submitted to *Phys. Rev. D*).
30. K. Woschnagg *et al.* (The AMANDA Collaboration), to appear in Proceedings of 21st International Conference on Neutrino Physics and Astrophysics (Neutrino 2004), Paris, France, 14-19 June 2004 (available from <arXiv:astro-ph/0409423>).
31. J. Ahrens *et al.* (The ICECUBE Collaboration), *Astropart. Phys.* **20**, 507 (2004) (available from <arXiv:astro-ph/0305196>).
32. A. Heijboer *et al.* (The ANTARES Collaboration), in Proceedings of 28th International Cosmic Ray Conference (ICRC 2003), Tsukuba, Japan, 31 July - 7 August 2003, p.1321.
33. C. Distefano, D. Guetta, E. Waxman and A. Levinson, *Astrophys. J.* **575**,

- 378 (2002) (available from <arXiv:astro-ph/0202200>).
34. Zh.-A. M. Djilkibaev *et al.* (The BAIKAL Collaboration), to appear in Proceedings of 21st International Conference on Neutrino Physics and Astrophysics (Neutrino 2004), Paris, France, 14-19 June 2004.
 35. M. Ambrosio *et al.* (The MACRO Collaboration), *Astropart. Phys.* **20**, 1 (2003) (available from <arXiv:astro-ph/0203181>).
 36. W. Rhode *et al.* (The FREJUS Collaboration), *Astropart. Phys.* **4**, 217 (1996).
 37. J. Ahrens *et al.* (The AMANDA Collaboration), *Phys. Rev. Lett.* **92**, 071102 (2004) (available from <arXiv:astro-ph/0309585>).
 38. E. Waxmann and J. N. Bahcall, *Phys. Rev.* **D59**, 023002 (1999) (available from <arXiv:hep-ph/9807282>).
 39. K. Mannheim, R. J. Protheroe and J. P. Rachen, *Phys. Rev.* **D63**, 023003 (2001) (available from <arXiv:astro-ph/9812398>).
 40. M. Ambrosio *et al.* (The MACRO Collaboration), *Phys. Rev.* **D60**, 082002 (1999) (available from <arXiv:hep-ex/9812020>).
 41. O. V. Suvorova, in Proceedings of 2nd International Conference on Physics Beyond the Standard Model: Accelerator, Nonaccelerator and Space Approaches (Beyond the Desert 1999), Ringberg Castle, Tegernsee, Germany, 6-12 June 1999, p.853 (available from <arXiv:hep-ph/9911415>).
 42. S. Desai *et al.* (The SUPER-KAMIOKANDE Collaboration), *Phys. Rev.* **D70**, 083523 (2004), **erratum:** *ibid.* **D70**, 109901 (2004) (available from <arXiv:hep-ex/0404025>).
 43. A. H. Chamseddine, R. Arnowitt and P. Nath, *Phys. Rev. Lett.* **49**, 970 (1982); R. Barbieri, S. Ferrara and C. A. Savoy, *Phys. Lett.* **B119**, 343 (1982); L. J. Hall, J. Lykken and S. Weinberg, *Phys. Rev.* **D27**, 2359 (1983).
 44. See URL <http://www.km3net.org>